Research Paper
J. Astron. Space Sci. 36(2), 61-68 (2019)
https://doi.org/10.5140/JASS.2019.36.2.61

JASS Journal of Astronomy and Space Sciences

Seasonal and Local Time Variations of Sporadic E Layer over South Korea

Eunbyeol Jo[1], Yong Ha Kim[1†], Suin Moon[1], Young-Sil Kwak[2]

[1]Dept. Astronomy, Space Science and Geology, Chungnam National University, Daejeon 34134, Korea
[2]Korea Astronomy and Space Science Institute, Daejeon 34055, Korea

We have investigated the variations of sporadic E (Es) layer using the measurements of digisondes at Icheon (37.14°N, 127.54°E, IC) and Jeju (33.4°N, 126.30°E, JJ) in 2011–2018. The Es occurrence rate and its critical frequency (*foEs*) have peak values in summer at both IC and JJ in consistent with their known seasonal variations at mid-latitudes. The virtual height of the Es layer (*h'Es*) during equinox months is greater than that in other months. It may be related to the similar variation of meteor peak heights. The *h'Es* shows the semidiurnal variations with two peaks at early in the morning and late in the afternoon during equinoxes and summer. However, the semi-diurnal variation is not obvious in winter. The semi-diurnal variation is generally thought to be caused by the semi-diurnal tidal variation in the neutral wind shear, whose measurements, however, are rare and not available in the region of interest. To investigate the formation mechanism of Es, we have derived the vertical ion drift velocity using the Horizontal Wind Model (HWM) 14, International Geomagnetic Reference Field, and Naval Research Laboratory Mass Spectrometer and Incoherent Scatter Radar-00 models. Our results show that *h'Es* preferentially occur at the altitudes where the direction of the vertical ion velocity changes. This result indicates the significant role of ion convergence in the creation of Es.

Keywords: ionosphere, sporadic E, ionosonde, semidiurnal tide

1. INTRODUCTION

Sporadic E (Es) represents a thin layer of enhanced electron density in the ionospheric E region. The electron density at Es is 2–3 times greater than that of surrounding and even reaches to 10^{12} m^{-3}. The Es layer has a thickness of about 1–2 km and its horizontal length is tens to hundreds of km (Maeda & Heki 2014). In mid-latitudes, the Es layer is formed when the long-lived metallic ions ablated from meteors are converged by horizontal neutral wind shear (Chu et al. 2014; Yeh et al. 2014). The thin Es layer affects radio propagation, and thus hampers to monitor the ionosphere from ground-based GNSS receivers (Hong et al. 2017).

In mid-latitudes, the occurrence rate and intensity (peak frequency, *foEs*) of Es layers display the typical seasonal variations; they are maximal in summer (e.g. Kelley 2009 and references therein). This phenomenon is explained by the maximal influx of meteors in summer (Haldoupis et al. 2007). However, it cannot explain why the occurrence rate is not increasing during the Geminids (a meteor shower from Gemini constellation) in the northern hemispheric winter, even though the meteor influx increases during this period. It may be because metallic ions diverge in the E region by the horizontal neutral wind in the ionospheric E region during this period (Yeh et al. 2014). The convergence of metallic ions by wind shear leads to the high occurrence rate of Es in summer, whereas the Es layer is difficult to be formed in winter in spite of abundant metallic ions because of the divergence of horizontal neutral winds. The wind shear also causes the local time variation of Es height as well as the seasonal variations of the Es intensity and occurrence rate. The semidiurnal variation of the Es height in all seasons

Received 23 APR 2019 **Revised** 23 MAY 2019 **Accepted** 27 MAY 2019
†**Corresponding Author**
Tel: +82-42-821-5467, E-mail: yhkim@cnu.ac.kr
ORCID: https://orcid.org/0000-0003-0200-9423

in midlatitudes is attributed to the semidiurnal variation of the wind shear driven by atmospheric tides (Chu et al. 2014; Oikonomou et al. 2014).

Moreover, the occurrence and intensity of Es is also known to be affected by an intermediate descending layer (IDL), diurnal or terdiurnal tides (e.g. Haldoupis et al. 2006; Oikonomou et al. 2014), non-migrating tide (Shinagawa et al. 2017), lightning (Yu et al. 2015), spread F (Haldoupis et al. 2003; Lee & Chen 2018), and nighttime medium-scale traveling ionospheric disturbances (Otsuka et al. 2008; Ogawa et al. 2009). The IDL is a layer between F1 and E layers which occurs irregularly (Haldoupis 2012). These additional sources of the Es generation complicate the seasonal and local time variations of measured Es parameters.

According to Zhang et al. (2015), in the mid-latitudes, the correlation coefficient between the solar activity and the Es intensity is positive and negative during day and night time, respectively. Moreover, they noted that the electron density of the Es layer increases after the geomagnetic disturbance. Zhou et al. (2017) also reported that the critical frequency of sporadic E (*foEs*) tends to be larger during the high geomagnetic activity. However, there are also several studies suggesting that the solar and geomagnetic activities do not affect the Es occurrence (Tan et al. 1985; Pietrella et al. 2014). Thus, the Es occurrence and its temporal variation are still not understood in detail, and there may be local effects to be identified.

Despite continuing ionosonde operation in Korea since 1960's, there has been no study on the Es layer using the Korean ionosonde data. Although it is expected that the Es layer over Korean peninsula follows typical mid-latitude characteristics, it is needed to confirm or disconfirm the characteristics at a quantitative level by using the locally measured data. In this paper, we report the first analysis results of Es layer data measured by ionosondes at Icheon and Jehu. Our analysis focuses on the season and local time variations of Es occurrence and intensity. In addition, to discuss the relation between the vertical ion drift convergence and Es layer height, we compared measured heights of Es layer with the vertical ion drift velocity profiles driven by the horizontal neutral wind which was calculated from the Horizontal Wind Model (HWM)-14 International Geomagnetic Reference Field (IGRF12), and Naval Research Laboratory Mass Spectrometer and Incoherent Scatter Radar (NRLMSISE)-00 model.

2. DATA

Ionosondes measure the critical frequencies of ionized layers in ionosphere and their virtual heights routinely day and night. The sporadic E data used in this study were obtained from the ionosonde measurements at Icheon (37.14°N, 127.54°E, IC) and Jeju (33.4°N, 126.30°E, JJ) in 2011–2018. The ionosondes carry out the vertical incidence observation with a time interval of 15 min as well as the oblique incidence observation between Korea and Japan. We used only vertical incidence data. Table 1 shows the number of available ionograms at IC and JJ. Fig. 1(a) and 1(b) show typical ionograms without and with a sporadic E layer, respectively, measured at IC. The sporadic E layer clearly appears as a thin layer of echo signals at the bottom of Fig. 1(b). To investigate the occurrence rate of the Es layer, we calculated the Es occurrence rate as follows:

$$\text{Occurrence rate} = \frac{\text{The number of } E_S \text{ ionograms per day}}{\text{The number of total ionograms per day}} \quad (1)$$

The IC and JJ ionosondes are a type of the digisonde, Digisonde Portable Sounder 4D (DPS4D). The observations of the ionosondes are analyzed by a software of Automatic Real-Time Ionogram Scaling with True analysis (ARTIST-5) and then saved as a format of Standard Archiving Output (SAO). The auto-scaled data can be downloaded at the website of the Korean Space Weather Center (http://spaceweather.rra.go.kr/). Although the Jeju auto-scaled F2 parameters were evaluated to differ by 36% from manually scaled ones (Jeong et al. 2018), the auto-scaled Es parameters are expected to be more accurate than the auto-scaled F2 parameters since the Es layer is significantly easy to be defined automatically.

3. RESULTS AND DISCUSSION

Fig. 2 displays the seasonal variations of the Es occurrence rate at IC (black line) and JJ (red line). The occurrence rate on each day is obtained using the data in 2011 –2018. In Figs. 2(a) and 2(b), the Es occurrence rate and the magnitude of

Table 1. The number of available ionograms measured by the Icheon (IC) and Jeju (JJ) ionosondes during a period of 2011–2018

Year	IC	JJ
2011	34,083	33,338
2012	32,469	33,629
2013	34,336	31,173
2014	31,991	33,031
2015	34,164	33,673
2016	34,123	33,021
2017	34,790	33,350
Total	34,351	32,275

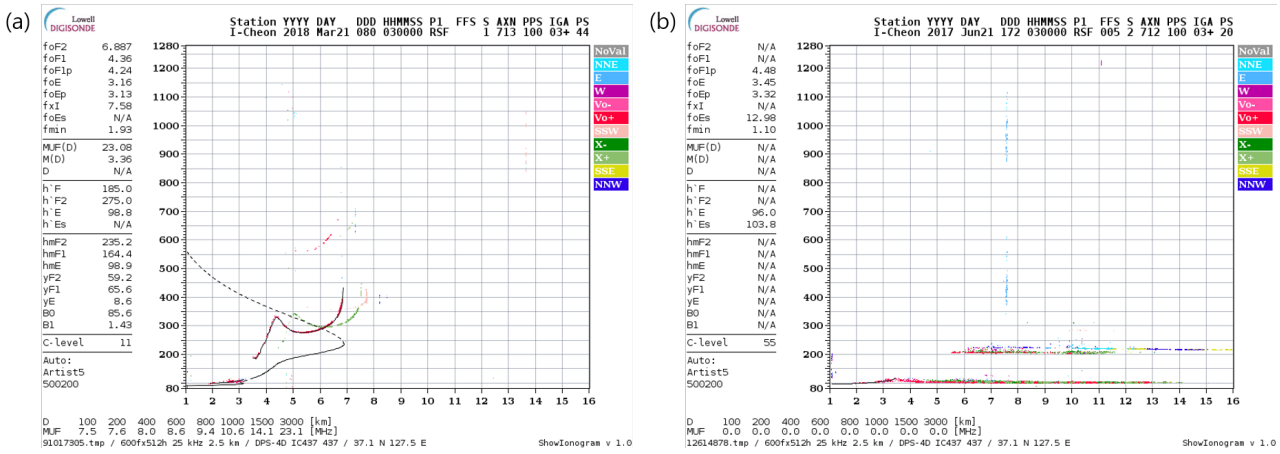

Fig. 1. (a) An example of a normal ionogram (no sporadic E layer), (b) an ionogram with a sporadic E layer measured at Icheon station.

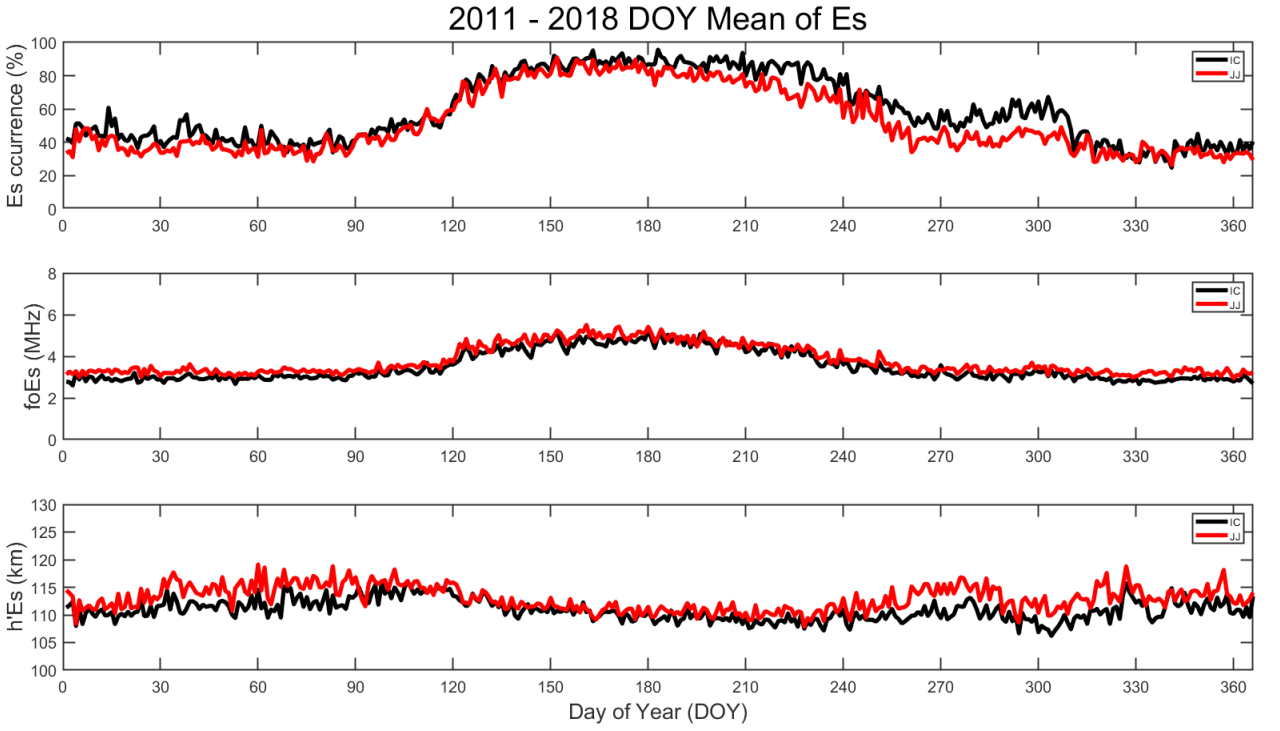

Fig. 2. Seasonal variations of the Es observed during the year of 2011–2018 at Icheon (black line) and Jeju (red line). The X-axis and Y-axis are the day of year and the occurrence rate, respectively.

foEs have the peak values in summer season in consistent with their known seasonal pattern in midlatitudes (Haldoupis 2012). This behavior is related to the wind shear and meteor influx in summer (Haldoupis et al. 2007; Arras et al. 2008; Chu et al. 2014; Yeh et al. 2014). However, the virtual height of Es (*h'Es*) shows the semiannual variation at both IC and JJ with two peaks in equinoxes (Fig. 2c). Meteor radar measurements have reported that peak altitudes of meteors vary in a similar manner around the mesopause altitude (Lee et al. 2016). The meteor peak variation is interpreted as a consequence of seasonal geopotential height change. The seasonal variation of *h'Es* may be related to the meteor peak height variation since the atmospheric change around the mesopause will affect the background atmosphere at the Es layer. Further investigation is needed to test the relation between variation of *h'Es* and meteor peak heights.

Maps of Es occurrence rate as a function of time and height at IC and JJ are shown in Figs. 3 and 4, respectively.

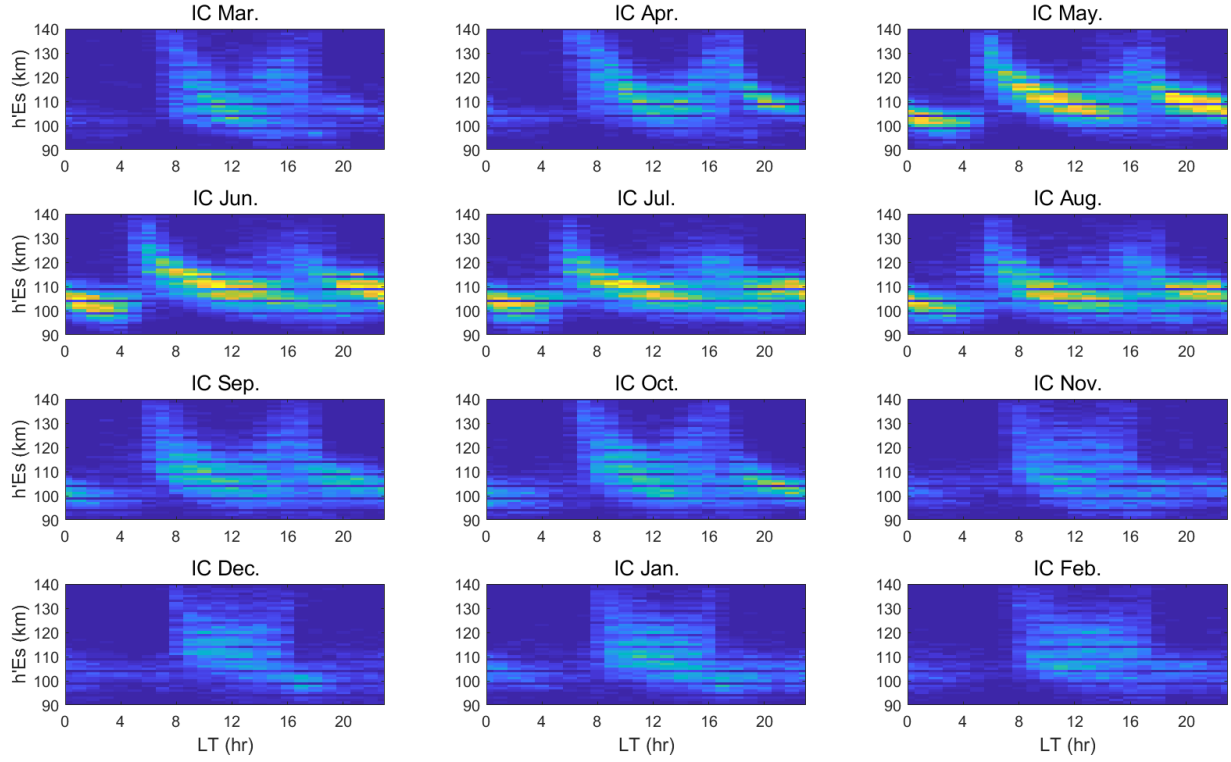

Fig. 3. Monthly height-time-occurrence rate of Es at Icheon.

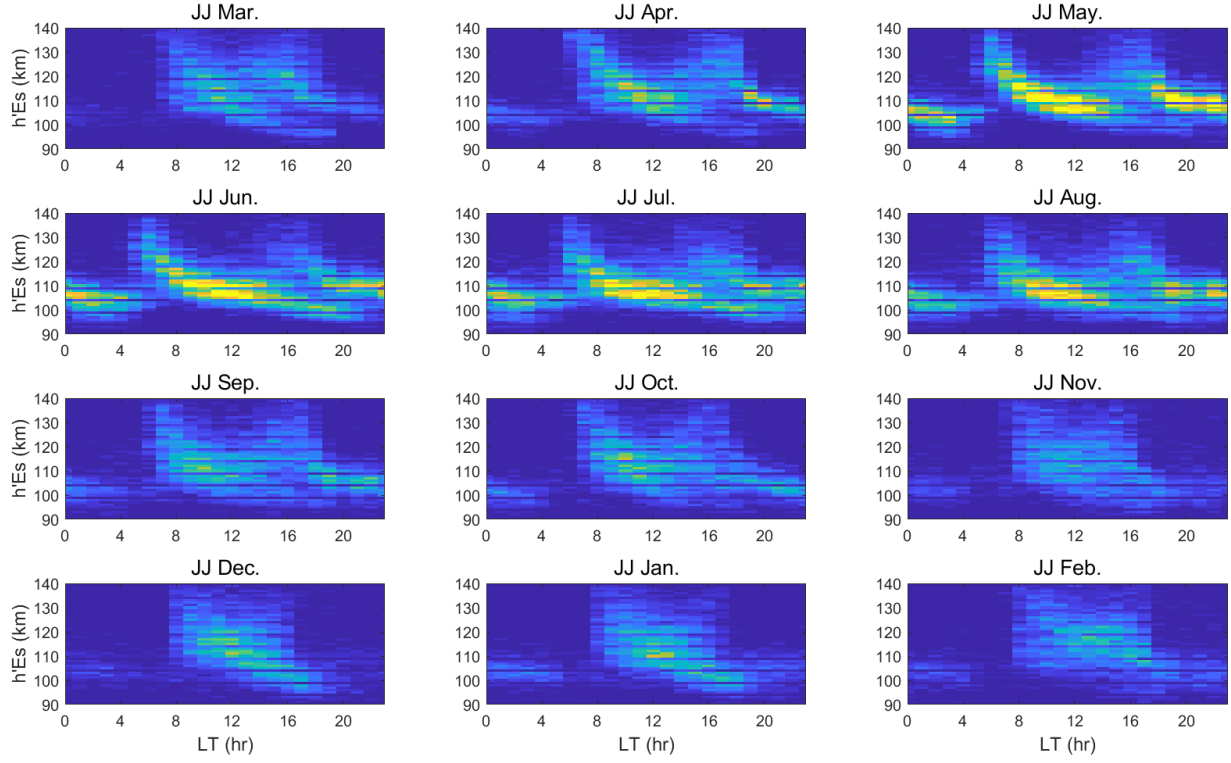

Fig. 4. Monthly height-time-occurrence rate of Es at Jeju.

The time and height bins of the plot are 1 hour and 1 km. In both IC and JJ, *h'Es* shows a semi-diurnal variation that has two distinct peaks at early morning and the other at late afternoon. The semi-diurnal variation is most pronounced in summer, but the two peaks are not obvious in winter. Similar phenomena were identified at different regions (e.g. Chu et al. 2014; Oikonomou et al. 2014).

Theoretical studies have proposed a scenario that the Es layer is formed when the metallic ions are converged by the neutral wind shear in the mid-latitudes (e.g. Chu et al. 2014). Fig. 5(a) illustrates the Es layer formation by the zonal wind shear. When the eastward zonal wind blows, the ions are vertically upward drifted by $\vec{U}\times\vec{B}$ where $\vec{U}$ is zonal wind velocity and $\vec{B}$ is geomagnetic field. In contrast, the westward zonal wind drifts the ions downward. In addition, the ion-neutral collision is frequent in the ionospheric E region because of the high atmospheric density, so that the meridional wind can move the ions along the geomagnetic field line. For example, in the northern hemispheric mid-latitudes, the meridional wind moves the ions as shown in Fig. 5(b), thus the Es layer forms by the ion convergence (Chen et al. 2010; Haldoupis 2012; Yeh et al. 2014). In the geomagnetic equatorial region, the geomagnetic field lines are almost parallel to the horizontal, so that the meridional wind can only move ions easily along the lines. On the other hand, the zonal wind can move ions vertically by $\vec{U}\times\vec{B}$. However, the zonal wind cannot easily form the Es layer because ions are fixed to the geomagnetic field lines in the E-region altitudes, where the ion- neutral collisional frequency is much greater than the ion gyro-frequency. In the high-latitudes, the horizontal component of the geomagnetic field lines is too small to form the Es layer by zonal and meridional wind. Therefore, the Es formation by wind shear is difficult in the geomagnetic equatorial and high-latitude regions.

Following the formula in Mathews (1998), the vertical ion drift velocity (w) can be expressed as a function of the zonal and meridional wind velocities,

$$w = \frac{\left(\frac{\nu_i}{\omega_i}\right)\cos(I)}{1+\left(\frac{\nu_i}{\omega_i}\right)^2}U + \frac{\cos(I)\sin(I)}{1+\left(\frac{\nu_i}{\omega_i}\right)^2}V \tag{2}$$

where U and V are the zonal and meridional wind velocities, respectively. Note that eastward zonal wind velocity is set to be positive, and I is the dip angle calculated from the IGRF. ν_i/ω_i is the ratio of the ion-neutral collision frequency to the ion gyro-frequency, which can be calculated by the Eqs. (3) and (4) (Yuan et al. 2014).

$$\frac{\nu_i}{\omega_i} = \frac{m_+\nu_\varepsilon}{eB_0} \tag{3}$$

$$\nu_\varepsilon = \left[\frac{1.80}{\sqrt{A(A+28)}}n_{N_2} + \frac{1.83}{\sqrt{A(A+32)}}n_{O_2} + \frac{1.80}{\sqrt{A(A+16)}}n_O\right]\times 10^{-14} \tag{4}$$

where m_+ is the average ion mass, e and B_0 are electron charge and magnetic field, A is the metallic ion mass, n_{N_2}, n_{O_2}, and n_O are the number densities of N_2, O_2, and O, respectively. The meridional wind term can be neglected in the Eq. (2) because of $\nu_i \gg \omega_i$ below the altitude of 120 km. Thus the vertical ion drift velocity is mainly controlled by the zonal wind term in the ionospheric E region.

In this study, we investigated the correlation between the gradient of the vertical ion drift velocity with the altitude *dw/dz* and the *h'Es*. To compute the vertical ion drift velocity profile, we adopted neutral densities from the NRLMSISE-00, and the neutral winds from the HWM14. When the eastward

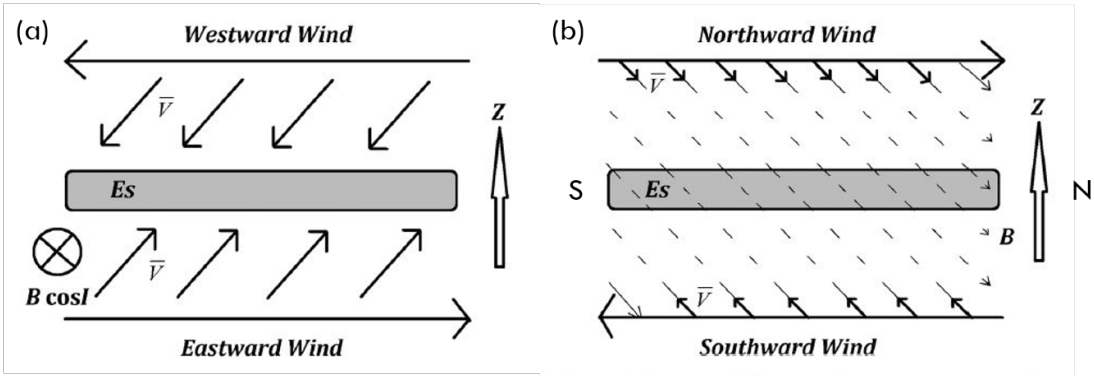

Fig. 5. Illustration of the wind shear convergence mechanism for ions in the northern hemisphere (Yeh et al. 2014). (a) The *Es* layer formation by the zonal wind shear. (b) The *Es* layer forms by the meridional wind shear.

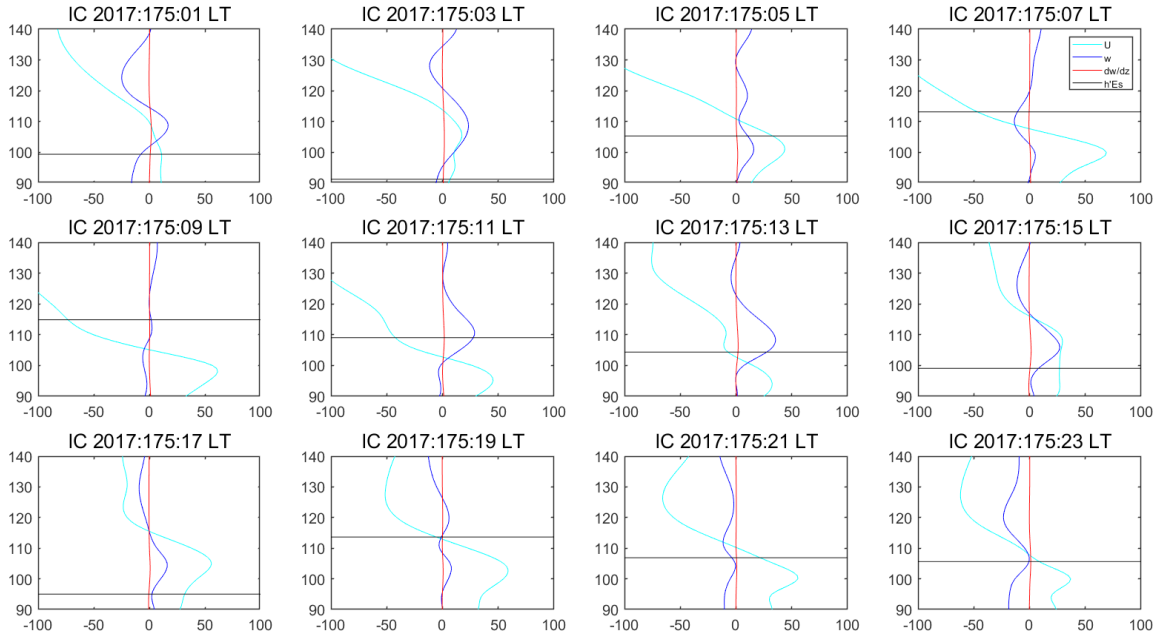

Fig. 6. Vertical profiles of the zonal wind velocity (cyan), vertical ion drift velocity (blue), and *dw/dz* (red) from 90 to 140 km, and *h'Es* (black) at IC in the day of June 24, 2017. The numbers in x-axis are in units of m/s and $10^{-3}s^{-1}$ for wind and drift velocities, and *dw/dz*, respectively.

and westward winds are blowing at low and high altitudes, respectively, as shown in Fig. 5(a) the *dw/dz* is negative. That is, the $dw/dz < 0$ represents the ion convergence, whereas the $dw/dz > 0$ means the ion divergence.

Fig. 6 shows the profiles of the zonal wind velocity (U), vertical ion drift velocity (w), and *dw/dz*, which are calculated from 90 to 140 km, and the 1 hour mean *h'Es* at IC on the day of June 24, 2017. The cyan, blue, red, and black lines are the U, w, *dw/dz*, and *h'Es*, respectively. The Es layers appear under the altitude of 100 km from midnight until dawn (01–04 LT), which may not be related to the vertical ion drift because the ionospheric E region normally disappears at nighttime due to fast recombination of molecular ions produced during daytime. The Es layers may be caused by *in situ* meteor ablation and survive because of slow recombination of metal atomic ions (Fe^+, Mg^+, Na^+) (see Kelley 2009). After 04 LT, except 14–17 LT, the Es layers occur around the altitude where the *dw/dz* is minimum, that is, the vertical ion convergence is maximum. During 14–17 LT, the Es layers tend to form around where the first (lower altitude) minimum of *dw/dz*. The local time variations of the profiles and *h'Es* at JJ are similar to the Fig. 6. Therefore, the semidiurnal variation of *h'Es* is related to the variation of vertical ion drift which was driven by semidiurnal tide of neutral winds. However, the nighttime Es occurrence, especially from midnight to dawn, is not consistent with the vertical ion drift.

4. CONCLUSIN AND SUMMARY

We have investigated the occurrence climatology of Es using the measurements of ionosondes at IC and JJ in 2011-2018. In both stations, the occurrence rate of Es and the magnitude of *foEs* show the maximum values in summer, confirming previous studies of mid-latitude Es (Haldoupis et al. 2007; Chu et al. 2014; Yeh et al. 2014). However, the *h'Es* shows semi-annual variation with two peaks in equinox months, similar to that of meteor peak heights in the mesosphere measured by a meteor radar at King Sejong Station (Lee et al. 2016). The local time variations of the *h'Es* shows the semidiurnal modulation during equinox months and summer months, which is consistent with the results in previous studies (e.g. Haldoupis et al. 2006; Oikonomou et al. 2014). However, the semi-diurnal variation is not obvious in winter. Our calculation of the vertical ion velocity using HWM14, IGRF12, and NRLMSISE-00 models support the association of the semidiurnal variation of *h'Es* with the semidiurnal variation of tidal horizontal wind.

ACKNOWLEDGEMENTS

The ionosonde data is provided by Korea Space Weather Center (http://spaceweather.rra.go.kr/). The work is financially supported by a project from Korea Astronomy

and Space Science Institute as a part of Korea ionosphere prediction model development by Korea Space Weather Center. Y.-S. Kwak was also supported by Air Force Office of Scientific Research (AFOSR)/Asian Office of Aerospace Research and Development (AOARD) grant FA2386-18-1-0107.

REFERENCES

Arras C, Wickert J, Beyerle G, Heise S, Schmidt T, et al., A global climatology of ionospheric irregularities derived from GPS radio occultation, Geophys. Res. Lett. 35, L14809 (2008). https://doi.org/10.1029/2008GL034158

Chen G, Zhao Z, Yang G, Zhou C, Yao M, et al., Enhancement and HF Doppler observations of sporadic–E during the solar eclipse of 22 July 2009, J. Geophys. Res. 115, A09314 (2010). https://doi.org/10.1029/2010JA015530

Chu YH, Wang CY, Wu KH, Chen KT, Tzeng KJ, et al., Morphology of sporadic E layer retrieved from COSMIC GPS radio occultation measurements: Wind shear theory examination, J. Geophys. Res. 119, 2117-2136 (2014). https://doi.org/10.1002/2013JA019437

Haldoupis C, Kelley MC, Hussey GC, Shalimov S, Role of unstable sporadic–E layers in the generation of midlatitude spread F, J. Geophys. Res. 108, 1446 (2003). https://doi.org/10.1029/2003JA009956

Haldoupis C, Midlatitude sporadic E. A typical paradigm of atmosphere-ionosphere coupling, Space Sci. Rev. 168, 441-461 (2012).

Haldoupis C, Meek C, Christakis N, Pancheva D, Bourdillon A, Ionogram height–time–intensity observations of descending sporadic E layers at mid-latitude, J. Atmos. Sol. Terr. Phys. 68, 539-557 (2006). https://doi.org/10.1016/j.jastp.2005.03.020

Haldoupis C, Pancheva D, Singer W, Meek C, MacDougall J, An explanation for the seasonal dependence of midlatitude sporadic E layers, J. Geophys. Res. 112, A06315 (2007). https://doi.org/10.1029/2007JA012322

Hong J, Kim YH, Chung JK, Ssessanga N, Kwak, YS, Tomography reconstruction of ionospheric electron density with empirical orthonormal functions using Korea GNSS network, J. Astron. Space Sci. 34, 7-17 (2017). https://doi.org/10.5140/JASS.2017.34.1.7

Jeong, SH, Kim YH, Kim K, Manual scaling of ionograms measured at Jeju (33.4°N, 126.3°E) throughout 2012, J. Asrton. Space Sci. 35, 143-149 (2018). https://doi.org/10.5140/JASS.2018.35.3.143

Kelley, MC, The Earth's Ionosphere: Plasma Physics and Electrodynamics. 2nd ed. (Academic Press, London, 2009), 284.

Lee CC, Chen WS, Effects of sporadic E-layer characteristics on spread-F generation in the nighttime midlatitude ionosphere: A climatological study, J. Atmos. Sol. Terr. Phys. 169, 130-137 (2018). https://doi.org/10.1016/j.jastp.2018.02.002

Lee C, Kim JH, Jee G, Lee W, Song IS, et al., New method of estimating temperatures near the mesopause region using meteor radar observation, Geophys. Res. Lett., 43, 10580-10585 (2016) doi:10.1002/2016GL071082

Maeda J, Heki K, Two–dimensional observations of mid-latitude sporadic E irregularities with a dense GPS array in Japan, Radio Sci. 49, 28-35 (2014). https://doi.org/10.1002/2013RS005295

Mathews JD, Sporadic E: Current views and recent progress, J. Atmos. Sol. Terr. Phys. 60, 413-435 (1998). https://doi.org/10.1016/S1364-6826(97)00043-6

Ogawa T, Nishitani N, Otsuka Y, Shiokawa K, Tsugawa T, et al., Medium–scale traveling ionospheric disturbances observed with the SuperDARN Hokkaido radar, all–sky imager, and GPS network and their relation to concurrent sporadic E irregularities, J. Geophys. Res. 114, A03316 (2009). https://doi.org/10.1029/2008JA013893

Oikonomou C, Haralambous H, Haldoupis C, Meek C, Sporadic E tidal variabilities and characteristics observed with the Cyprus Digisonde, J. Atmos. Sol. Terr. Phys. 119, 173-183 (2014). https://doi.org/10.1016/j.jastp.2014.07.014

Otsuka Y, Tani T, Tsugawa T, Ogawa T, Saito A, Statistical study of relationship between medium-scale traveling ionospheric disturbance and sporadic E layer activities in summer night over Japan, J. Atmos. Sol. Terr. Phys. 70, 2196-2202 (2008). https://doi.org/10.1016/j.jastp.2008.07.008

Pietrella M, Pezzopane M, Bianchi C, A comparative sporadic-E layer study between two mid-latitude ionospheric stations, Adv. Space Res. 54, 150-160 (2014). https://doi.org/10.1016/j.asr.2014.03.019

Shinagawa H, Miyoshi Y, Jin H, Fujiwara H, Global distribution of neutral wind shear associated with sporadic E layers derived from GAIA, J. Geophys. Res. 122, 4450-4465 (2017). https://doi.org/10.1002/2016JA023778

Tan ZX, Huang XY, Wang S, A preliminary investigation of ionospheric Es-s over Wuchang, China, J. Atmos. Terr. Phys. 47, 959-963 (1985). https://doi.org/10.1016/0021-9169(85)90073-X

Yeh WH, Liu JY, Huang CY, Chen SP, Explanation of the sporadic–E layer formation by comparing FORMOSAT–3/COSMIC data with meteor and wind shear information, J. Geophys. Res. 119, 4568-4579 (2014). https://doi.org/10.1002/2013JD020798

Yu B, Xue X, Lu G, Ma M, Dou X, et al., Evidence for lightning–associated enhancement of the ionospheric

sporadic E layer dependent on lightning stroke energy, J. Geophys. Res. 120, 9202-9212 (2015). https://doi.org/10.1002/2015JA021575

Yuan T, Wang J, Cai X, Sojka J, Rice D, et al., Investigation of the seasonal and local time variations of the high–altitude sporadic Na layer (Nas) formation and the associated midlatitude descending E layer (Es) in lower E region, J. Geophys. Res. 119, 5985-5999 (2014). https://doi.org/10.1002/2014JA019942

Zhang Y, Wu J, Guo L, Hu Y, Zhao H, et al., Influence of solar and geomagnetic activity on sporadic-E layer over low, mid and high latitude stations, Adv. Space Res. 55, 1366-1371 (2015). https://doi.org/10.1016/j.asr.2014.12.010

Zhou C, Tang Q, Song X, Qing H, Liu Y, et al., A statistical analysis of sporadic E layer occurrence in the midlatitude China region, J. Geophys. Res. 122, 3617-3631 (2017). https://doi.org/10.1002/2016JA023135